

## MODEL STUDIES ON THE STRESS DISTRIBUTION IN LAYERED SOIL SYSTEMS

*By Koichi AKAI\*, Satoshi SHIOMI\*\* and Tsutomu KIUCHI\*\*\**

### 1. INTRODUCTION

Recently constructions of roads and runways are increasing with the remarkable development of the transportation facilities. Therefore it is requested to design these structures reasonably.

Pavements used today are, in general, divided into two kinds; concrete (rigid) pavement and asphalt (flexible) one. The design method of the former is based on Westergaard's theory derived from the theory of elasticity and, in this case, the load is supported mainly by the concrete slab. For the latter, on the other hand, there exists no reliable theory to be based on except the CBR method which has been found out by experiences. The CBR method is widely used in this country, nevertheless there are various design methods for the flexible pavement besides this. It can be said, therefore, that the basic theory for the flexible pavement has not been established.

In this point of view we may easily recognize the necessity of investigating the reliable pavement theory. The primary function of road or runway pavements is to spread loads from vehicle tires or airplane wheels into subgrade soils so that they do not cause shear failure or excessive deflection. The analysis of stress and deformation in the pavement system may, therefore, play an important role in the design procedure.

### 2. PREVIOUS RESEARCHES ON THE STRESS DISTRIBUTION IN SOIL

Adaptability of the well-known Boussinesq's theory to the real ground which corresponds to the static loading on a semi-infinite homogeneous elastic body was fully investigated by many researchers. The assumptions in this theory in principle are rarely satisfied in natural state. Nevertheless there

has occurred a question whether the theory would be available to the the ground at least as the first approximation. Mainly sands were tested, since it was comparatively easy to embed pressure-measuring devices in them.

In the remarkable test which was carried out by Kögler and Scheidig<sup>1)</sup> in 1927 an improved method of vertical-pressure measurement was employed. It consisted in using a very large number of pressure cells, which were placed so closely to each other that they formed continuous horizontal layers at several depths, thereby eliminating inaccuracies in the measurements due to differences in the compressibility of pressure cells and of surrounding sand.

It was noted from the test result that the vertical pressures in the sand were somewhat more concentrated under the footing and were less spread out laterally than is indicated by the Boussinesq's equations. Near the sand surface there existed a zone of zero stress, limited by the curve of zero pressure. The angle between that curve and the vertical equaled 35° near the sand surface, then increased gradually till at a certain depth was approached 90°.

This experiments performed by Kögler and Scheidig showed that the basic assumption of linear stress distribution under a loading plate could not be applicable to the actual ground. According to the summary by Kögler, the Boussinesq's equations have no value in the disturbed region of the loaded area, as we encounter with the road subgrade under a rigid loading plate.

The fundamental solution of stress distribution in a homogeneous, elastic, semi-infinite body is of unique value for a concentrated vertical load. When enlarging such a load to those on a plane, one has to integrate in respect with the individual load. Thus applying the law of superposition to the elastic semi-infinite body, the pressure distribution becomes to a concave parabola after Boussinesq and Schleicher<sup>2)</sup>; there occurs infinite stress at the rim of plate. As this is not acceptable a slight disturbance takes place at the rim, whereas the state of stress at the other region is not so influenced by this effect.

In his well-known study Fröhlich<sup>3)</sup> investigated to obtain better description of ground under the

\* Dr. Eng., Professor of Civil Engineering, Kyoto University

\*\* M.S.C.E., Civil Eng. Dept., Central Research Inst. of Electric Power Industry

\*\*\* M.S.C.E., Kumagai-Gumi, Co. Ltd., Osaka Branch

basis of linear transmission of stresses, which had to match to actual behaviors. In many experiments it was assumed that most soils have no tensile strength at their site. This can be truly said for fills, gravels and sands. Thus, introducing the concept of the stress concentration factor, he modified Boussinesq's formula to explain the above-mentioned stress distribution in ground. In his study Fröhlich confirmed that the research results by Kögler-Scheidig as well as the former investigators were in best coincidence with his new theory when one took the stress concentration factor  $\nu=6$ .

According to Ohde<sup>4)</sup> the conclusion is that the Boussinesq's theory as well as its extension by Fröhlich is of some value to foundation engineering. To be excepted is the region of disturbance under the loading plate. At the same time there exist some problems on measuring techniques on which various states of stress are to be verified.

In spite of assuming the soil as an elastic material it is very difficult to treat the two-layered and multi-layered problem mathematically. In road engineering we take a simplification into two-layered system; the upper layer and the underbase. Westergaard<sup>5)</sup> considered a semi-infinite homogeneous underbase and an overlying concrete slab, and computed stresses under a load. The vertical force is assumed to be proportional to the settlement. His work has originally confirmed the stress distribution in road subgrade under a rigid surface.

In 1943 there appeared the famous two-layered solution by Burmister<sup>6)</sup>. At first he established the boundary conditions, in which the solution of elasticity was applied. The conditions are either adhesive surface or frictionless surface between two layers. The deduction of solution was enlarged to evaluation of vertical displacement and to approximate application to three-layered problem two years later<sup>7)</sup>. The multi-layered problem has been treated by Odemark<sup>8)</sup> thereafter.

The visco-elastic behavior of road materials cannot be neglected in the rigorous design of subgrade structure. Layers combined by bituminous materials indicate some rheological properties. Assuming the linear viscoelasticity, approximate descriptions of time-dependent behaviors of such materials are performed theoretically. In order to use formulae introduced for purely elastic case, there is a possibility of Laplace transform by which the phenomenon is investigated on the transformed field<sup>9)</sup>. On this direction a series of researches has been established by Ishihara and Kimura<sup>10)</sup>. Of possibly even greater importance is for the case of periodic repeating loading on subgrade. Thus the design problem of such structures is orientated to the dynamic one.

### 3. MODEL STUDIES ON THE STRESS DISTRIBUTION

#### (1) General

It is understood that there exist three factors which affect stress distribution in soil as follows :

##### 1) Properties of soil

This means whether soil can be treated as elastic, isotropic, homogeneous material and continuum.

##### 2) Properties of loading plate

This means that the loading plate is a rigid plate or a flexible one, what is the shape and the scale of the plate.

##### 3) Properties of load

This means that the load is static or dynamic and, in case of the dynamic load, whether it is a pulse load or cyclic one and what is the form of the load.

It is, thus, of great importance to examine how these factors have an effect upon the stress distribution quantitatively. At first let us consider the factor 1).

It has been reported that, for cohesive soil, the measured stress agrees well with that computed by the theory of elasticity and, for cohesionless soil, the stress concentrates toward the axis of load. In case of sand and gravel which are regarded as cohesionless granular materials, the stress on the axis of load is beyond the capacity of the load intensity of materials with increase in load, and as the result, local fracture or slippage may occur on the neighbour of the axis of load. Therefore, the path of stress transmission may vary.

Next we come to the factor 2). It is with no doubt that the characteristics of stress distribution in soil are affected by what kind of load acts on it. That is, in other words, the problem of contact pressure and also of the boundary conditions. It has been generally reported that for the rigid loading plate, the settlement is equal at any point so that the contact pressure is presumed to be the form of concave parabola. It may be found that sand particles near the edge of the plate have no sharing resistance due to the lack of normal stress, so that they would yield and the stress would gradually begin to concentrate toward the axis of load. In case of cohesive soil, as it has cohesive strength, the shearing resistance is mobilized even if there exists no normal stress at all. It is supposed, therefore, that the stress would concentrate under the circumference of the rigid loading plate as anticipated by the theory of elasticity.

About the factor 3) it will be considered later in more detail.

## (2) Materials used

Three kinds of soil are used in the experiment, termed "sandy loam", "sand" and "gravel", respectively. Their physical properties are shown in Table 1 and the grain size distribution curves are in Fig. 1. From these curves the uniformity coefficient is 15.4 for sandy loam, 6.1 for sand and 8.0 for gravel.

**Table 1** Physical properties of soil materials

	Sandy loam	Sand	Gravel
Specific gravity	2.64	2.65	...
Clay fraction	0%	0%	0%
Silt fraction	20.5%	5.0%	1.0%
Sand fraction	76.5%	85.3%	13.0%
Gravel fraction	3.0%	9.7%	86.0%
Maximum grain size	9.52mm	9.52mm	19.1mm
Uniformity coefficient	15.4	6.1	8.0

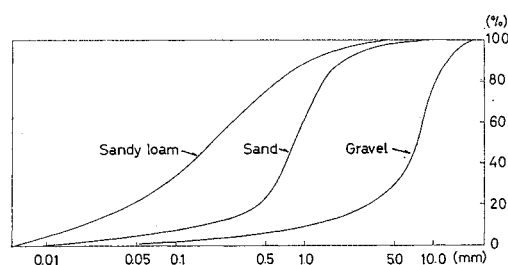


**Fig. 1** Grain size distribution curves.

The optimum moisture content of sandy loam is 11.8% approximately at which the layer was compacted. On the other hand, sand and gravel layers were compacted most densely. In order to minimize the variation in water content, the top of the test pit was sealed with a polyvinyl sheeting and water was sometimes sprinkled on the surface.

## (3) Test pit and loading system

The outline of the experimental apparatus is shown in Fig. 2 and Photo. 1. The test pit used in this work is 2m square in plan and 1.2m depth, and the materials are contained to the height of

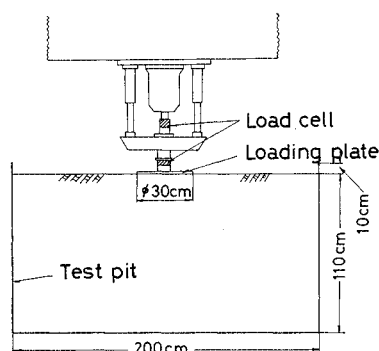


**Fig. 2** Experimental apparatus.

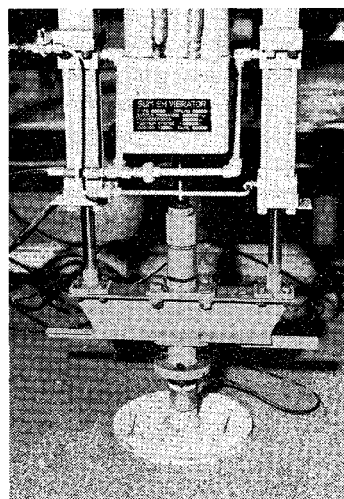


**Photo. 1** Dynamic loading apparatus.

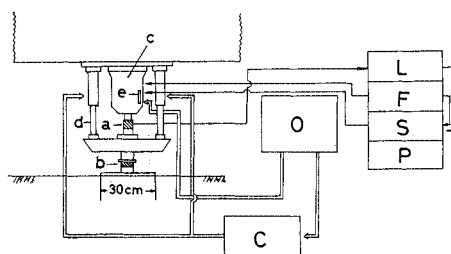


**Fig. 3** Loading system; a: load cell for control, b: load cell for measurement, c: cylinder for dynamic load, d: cylinder for sustained load, e: servo-valve, L: load amplifier, F: function generator, S: servo-amplifier, P: pressure source controller, O: oil pressure source, C: sustained pressure supporter.

1.05 m or 1.1 m from the bottom of the pit.

The loading system should be described in some detail as it was developed to apply both static and dynamic load on the soil medium. The outline of the loading system is shown in Fig. 3. The apparatus is operated by oil pressure and the loading system consists of the following parts.

The load producer consists of a vibrator (c) and two cylinders (d) for static load. The former is capable to apply the maximum load of 500 kg and the latter the maximum load of 1000 kg by each cylinder so that the maximum applied load amounts to 2500 kg by the whole loading system. The stroke of pistons is 10 cm.

The sustained pressure supporter (C) contains the accumulator in which nitrogen is filled in order to support the sustained load. The control console consists of four components: the load amplifier (L), the function generator (F), the servo-amplifier (S) and the pressure source controller (P). The load amplifier amplifies the signal from the load cell

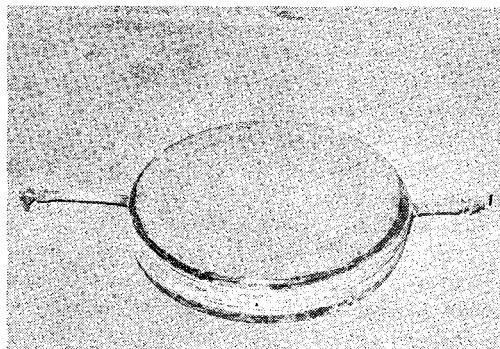
(a) to produce the feedback signal and directs the described static and dynamic load to the servo-amplifier. The function generator produces the wave form of load such as sinusoidal, triangular, square and sawtooth waves and can vary their frequencies from 0.01 cps to 100 cps. The servo-amplifier compares the deviation between the input signal voltage and the feedback signal one with each other and, if any deviation exists, it directs the servo-voltage so as to correct the deviation. The servo-valve which controls oil flow due to the signal from the servo-amplifier is connected with the vibrator through the oil tube.

Two kinds of loading plate were used; one was the rigid plate made of steel as shown in Photo. 2 (a) and the other was the flexible one made of rubber plate or rubber bag filled with water as indicated in Photo. 2 (b), thereby it was devised to produce a uniform circular load. The side of the rubber bag was reinforced by steel wires to maintain a given loaded diameter with the radius  $a=15$  cm.

An oil pressure jack was used to apply the load



(a)



(b)

Photo. 2 Loading plates; (a) rigid, (b) flexible.

on the soil mass. The maximum applied load was about 2 tons. When the rigid plate was used, the jack was put between the beam and the loading plate as shown in Fig. 4 (a), and was cramped to them to make unification as a loading system. When the flexible plate was used, on the other hand, it was put under the column used as the rigid plate as Fig. 4 (b).

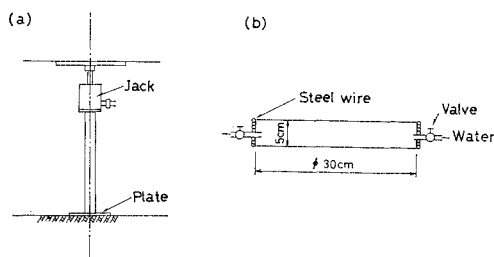


Fig. 4 Loading plates; (a) rigid, (b) flexible.

#### (4) Instrumentation

Two types of pressure cell were used in this experimental work. One was cylindrical, 8 cm diameter by 1.5 cm thickness, and the other was also cylindrical, 10 cm diameter by 2 cm thickness. Maximum capacity of these pressure cells was  $3 \text{ kg/cm}^2$ .

In addition to these pressure cells two dial gauges were used to measure the surface settlement and these are equipped on the loading plate symmetrically as shown in Photo. 3.

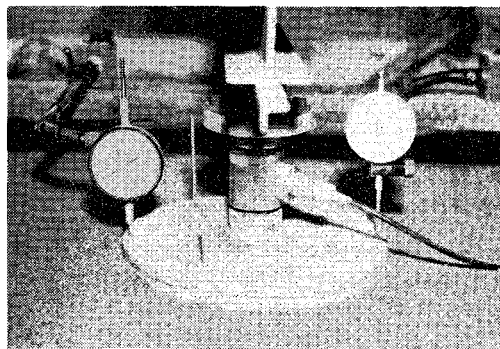


Photo. 3 Measurement of surface settlement.

#### (5) Instrument layout and installation

The layout of pressure cells is shown in Fig. 5. This pattern was repeated at various depths to measure

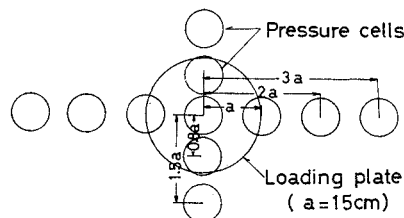


Fig. 5 Layout of pressure cells.

the stress distribution, that is, at the depth of  $z = 0.5a, 1a, 2a$  and  $3a$  bellow the soil surface, where  $a$  is the radius of loading plate and has a value of 15 cm.

On installing the pressure cells, the pressure-sensitive diaphragms were covered by fine sand of about 1 cm thickness to avoid false reading which might occur when gravels would directly touch the diaphragms.

## (6) Loading programme

### 1) Static loading

Testing was performed on two kinds of single-layered and on a two-layered soil system. Sand and sandy loam were used as single-layered materials, while two-layered systems consisted of sand or gravel as the upper layer and sandy loam as the lower layer, and the thickness of the upper layer was chosen as  $h = 0.5a, 1a$  or  $2a$ .

After all arrangement was completed, static loading tests were performed at first. The load was increased step by step to the average uniform pressure of  $1.14 \text{ kg/cm}^2$  which was defined as the applied force divided by the area of the loading plate ( $A = 706.5 \text{ cm}^2$ ). In this case each loading increment was set to be  $0.10 \text{ kg/cm}^2$  or  $0.15 \text{ kg/cm}^2$ . In each step the normal stress distribution and the surface settlement were measured by pressure cells and dial gauges, respectively. After reaching the value of  $1.14 \text{ kg/cm}^2$  the load was decreased stepwise in each decrement of  $0.2 \text{ kg/cm}^2$  or  $0.3 \text{ kg/cm}^2$ . This loading procedure was repeated four times for the rigid loading plate, and then using the flexible plate made of rubber, similar static test was repeated three times.

Stresses were picked up by the pressure cells buried in soil medium and the signals from them were amplified and recorded directly.

The value of the stress and the surface settlement obtained after the second loading were used in the later discussion of stress distribution and surface settlement. The reason is that the measured stress had a little hysteresis under the first cycle of loading mainly caused by non-homogeneity of soil compaction. This phenomenon, however, disappeared after the second cycle of loading.

### 2) Dynamic loading

The above-mentioned static test was followed by the dynamic one. The sustained load was applied by the average uniform pressure of  $0.45 \text{ kg/cm}^2$ , and then the dynamic loads of sinusoidal form with the stress amplitude of  $0.21 \text{ kg/cm}^2$  and the frequencies of 0.5 cps, 1 cps and 5 cps in sequence were followed. After a series of tests under this sustained load was over, the load level was increased to  $0.67 \text{ kg/cm}^2$  and the dynamic load was applied

by same procedure as before. The sustained load was raised up to the ultimate value of  $0.88 \text{ kg/cm}^2$ .

After the test for dynamic load of sinusoidal form the load was taken off and the dynamic load of quadratic form with the amplitude of  $0.21 \text{ kg/cm}^2$  and the frequency of 1 cps was applied under the sustained load above-mentioned. Since the purpose of this test was to examine the effect of difference between loading forms on the stress distribution, only the frequency of 1 cps was adapted in case of the quadratic loading form.

During the dynamic test stresses picked up by the pressure cells were recorded on the electromagnetic oscilloscope, whereas the surface settlement was measured by using the transducer which had the capacity of 10 mm.

The moisture content and the in-situ density of soil medium were measured in each test. These results are tabulated in Table 2.

Table 2 Moisture content and in-situ density of soil

	Sandy loam		Sand	
Moisture content (%)	7.6	7.8	2.6	2.8
In-situ density ( $\text{t/m}^3$ )	1.80	2.03	1.87	1.85

## (7) Representation of test results

All the measured stresses are divided by the mean contact pressure and are referred to as "normalized stresses". This normalized stresses are plotted in figures as  $\sigma/q$ . The objective of this normalization is to enable to compare the measured stresses among the tests carried out under different various conditions.

In the representation of dynamic load, the following terms; sustained load, dynamic load and total load, and also of stress; static stress, dynamic stress and total stress are used, respectively. These terms are defined by using the signification shown in Fig. 6 as follows.

The sustained load means the load applied statically and is designated by  $q_s$ . The dynamic load means the load deviating from the sustained load

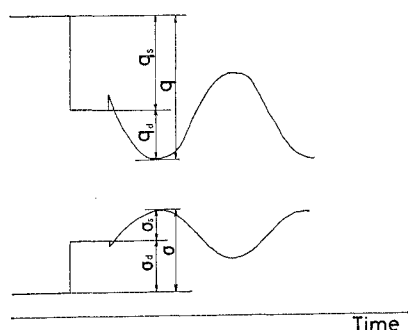


Fig. 6 Definition of load and stress.

and is designated by  $q_d$ . The total load means the sustained load plus the dynamic one and is designated by  $q$ , i.e.,  $q = q_s + q_d$ .

The static stress, the dynamic stress and the total stress which correspond to the sustained load, the dynamic load and the total load are designated by  $\sigma_s$ ,  $\sigma_d$  and  $\sigma = \sigma_s + \sigma_d$ , respectively. These stresses are also represented in the normalized form so that, for example, the dynamic stress denotes the ratio of  $\sigma_d/q$ .

#### 4. RESULT OF EXPERIMENT

##### (1) Static loading test

The result obtained for the single-layered system composed of sand is shown in Fig. 7 where the average values of stresses measured at each loading step with a rigid loading plate under static loading test and under sustained load only in dynamic loading test are plotted. The stress computed by the theory of elasticity for the semi-infinite, isotropic and homogeneous soil under a circular uniform load is drawn by a solid line. It may be found from this figure that the tendency of stress distribution in both cases is similarly developed, though the deviation between stresses measured in different test series is remarkably recognized.

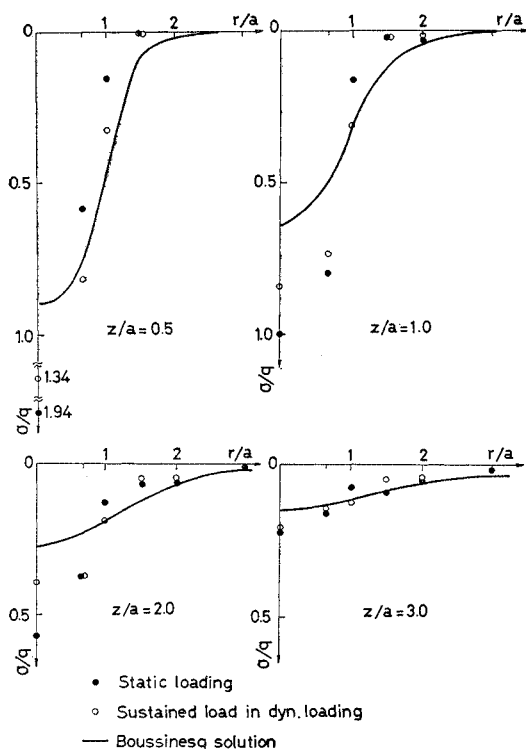


Fig. 7 Static stress distribution in sand layer under rigid loading plate.

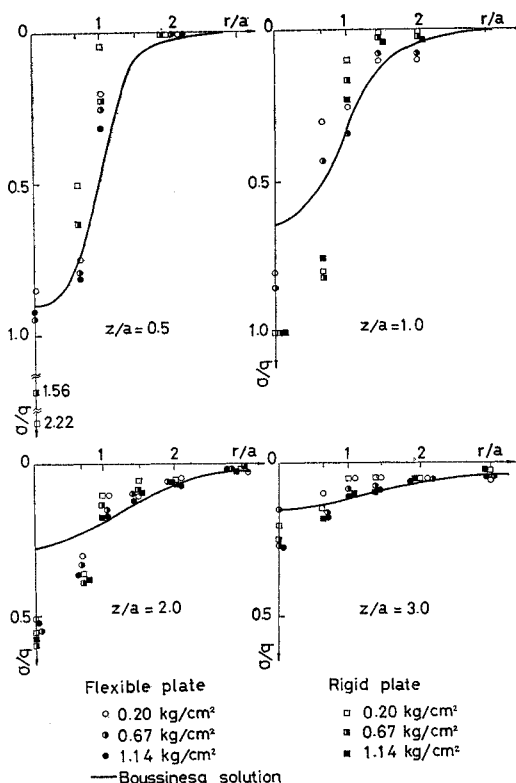


Fig. 8 Effect of load intensity and rigidity of loading plate on stress distribution in sand layer.

Fig. 8 is shown to examine the effect of load intensity and rigidity of the loading plate on the stress distribution. Stress distribution at the depth of  $z = 0.5a$  ( $a$ : the radius of loading plate) indicates distinctly the difference between the stress distribution due to the flexible loading plate and that due to the rigid one. Using the former, the measured stress coincides with theoretical solution. On the contrary, using the latter compelling the uniform displacement to the soil surface, the stress concentrates remarkably on the axis of load, which tendency is the same as reported by Kögler and his coworkers. The degree of stress concentration on the axis of load decreases with increase of applied load as shown in Table 3. The variation in stress with applied load, however, cannot be found when using the flexible loading plate. Therefore, the explanation of this phenomenon may be possible in assuming that the stress concentrating on the axis of load reaches the ultimate capacity of shearing resistance as the load increases and the sand near the axis of load is compacted by the occurrence of

Table 3 Degree of stress concentration on the axis of load

Load intensity $q$ (kg/cm <sup>2</sup> )	0.10	0.20	0.30	0.40	0.55	0.67
Stress ratio $\sigma/q$	2.20	2.22	2.10	1.99	1.84	1.56

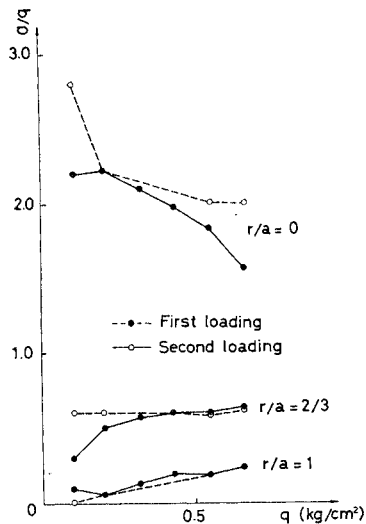


Fig. 9 Stress variation in sand layer due to increase of load intensity ( $z=0.5a$ ).

local slippage so that the sand beneath the loading plate is brought to charge greater load. The evidence of the above explanation is shown in Fig. 9, how stresses at any offset at the depth of  $z=0.5a$  vary as the load increases. This shows that the stress on the axis of load decreases with increase of the load intensity, while stresses at other positions have opposite tendencies. The stress outside the loading plate remains almost zero. It is concluded thus that the decrement in stress concentration on the axis of load as the load increases is not due to the extension of the range of charging the applied load but due to the increase in the degree of charging the load under the circumference. Using the flexible loading plate, the stress measured outside the loading plate is lower than the composed stress. It may be explained by lack of tensile strength of soil and also by absence of surcharge.

The result obtained for the single-layered system composed of sandy loam under the rigid loading plate, the pattern of stress distribution at the depth of  $0.5a$  becomes a little concave toward the axis of load as predicted by using the theory of elasticity. For the flexible loading plate made of rubber bag with water, on the other hand, the agreement between the stress distributions obtained by experiments and computed by using the Boussinesq's solution for uniform load is fairly good. Reaching the depth of  $2a$ , the rigidity of loading plate has no effect on the stress distribution.

To examine the characteristics of stress distribution on the horizontal plane, a comparison between the results obtained for three kinds of layer constitution is performed by using the average value of stresses measured at each loading step. The results

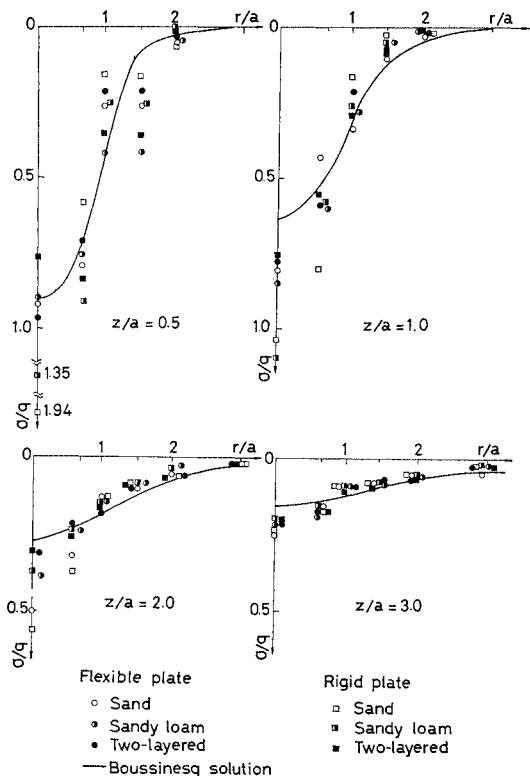


Fig. 10 Comparison between the stress distribution in sand, sandy loam and two-layered (sand/sandy loam) systems.

are shown in Fig. 10. It may be confirmed from this figure that, using the rigid loading plate, the stress in two-layered system indicates the mean value of the stress in sand and sandy loam at almost positions, whereas using the flexible plate, there exists no difference in stress distribution between three cases. It may be concluded, therefore, that the stress distributions at shallow depths in soil are more affected rather by the rigidity of loading plate than by the properties of soil used, while they are influenced only by soil properties at deep depths.

## (2) Dynamic loading test

### 1) Stress distribution

In order to make comparison between static stresses, dynamic stresses and total stresses, the applied load was varied in the following factors:

- Frequencies of the dynamic load—0.5 cps, 1 cps and 5 cps.
- Sustained loads—the mean contact pressures of 0.45 kg/cm<sup>2</sup>, 0.67 kg/cm<sup>2</sup> and 0.88 kg/cm<sup>2</sup>.
- Wave forms of dynamic load—the sinusoidal wave and the rectangular one.

The stress measured under the dynamic load of sinusoidal wave is shown in Fig. 11, in which (a), (b) and (c) correspond to the cases of sand, sandy

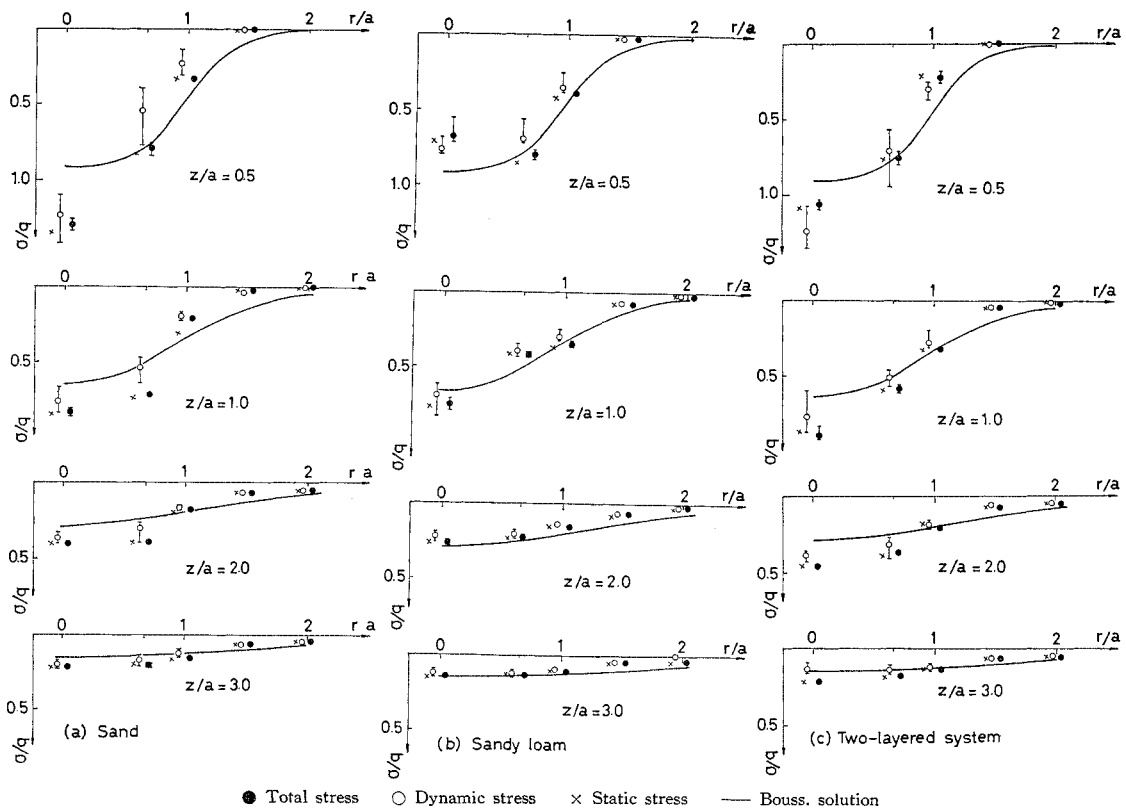


Fig. 11 Comparison between total stress, dynamic stress and static stress.

loam and the two-layered system, respectively, and the marks of closed circle and open circle designate the averages of total stresses and dynamic stresses, respectively. To study the relative magnitude of stresses at different depths all the results are plotted to the same vertical scale. The static stress is designated by the black mark (x) in the same figures to compare them. We can draw some characteristics in comparison between these figures as follows:

- i. The scattering range of dynamic stresses is much wider, in particular, for the layer consisting of sand.
  - ii. The total stress exhibits equal to or little smaller value than the static one except that at the depth of  $z=0.5a$  in the two-layered system. The tendency for the dynamic stress becomes more remarkable.
- 2) Effect of the frequency of load on stress distribution

Generally speaking, cohesive soils are more affected by the rate of loading than cohesionless soils. Sparrow and Tory<sup>11)</sup> showed that stresses were independent of the rate of loading, while Brown and Pell<sup>12)</sup> reported a slight increase in stress with the rate of loading, although this trend was much less pronounced than that for contact pressure.

For single-layered soil system the variation in the vertical normal stress with the frequency of load is not found within the cycle range treated in the present test, *i.e.*, from 0.5 cps to 5 cps.

The stress distribution in two-layered (sand/sandy loam) system is shown in Fig. 12 with respect to the frequency of load for the sustained load  $q_s = 0.45 \text{ kg/cm}^2$ . This indicates that the stress distribution in the two-layered system is similar to that in the sand single layer than in the sandy loam layer. This can be explained as follows. The stress has no trend to concentrate greatly on the axis of load at the depth of  $z=2a$ . Second, sandy loam used as the material for the lower layer has some viscosity so that the layer behaves like a rigid body under the dynamic load. This is proved by the extreme dispersion of stresses at the depth of  $z=3a$ .

3) Effect of sustained load on stress distribution

The effect of sustained load on stress distribution is hardly recognized except at the shallowest depth of  $z=0.5a$ . At the depth of  $0.5a$  the stress on the axis of load decreases with the increase of sustained load. As the same phenomenon is recognized in the static test, however, this may not be only due to the effect of dynamic loading.

Now let us consider the results for two-layered system consisting of gravel for the upper layer and



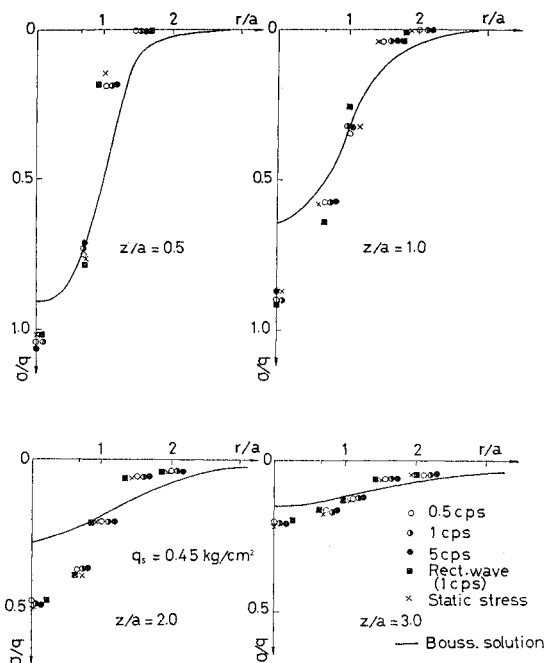


Fig. 12 Stress variation in two-layered (sand/sandy loam) system due to the frequency of dynamic loading ( $q_s = 0.45 \text{ kg/cm}^2$ ).

sandy loam for the lower layer. The stress distribution at the depth of  $z = 0.5a$  obtained by the static loading test is shown in Fig. 13 for each thickness of the upper layer,  $h = 0.5a$ ,  $1a$  and  $2a$ . Though the errors in the measurement are fairly large at this shallow depth, a remarkable effect of the thickness of upper layer on the stress spreading is seen. It is shown in this figure that the rigidity of loading plate affects slightly the stress distribu-

tion.

The comparison of the stress distribution for gravel/sandy loam system with that for sand/sandy loam system indicates that the tendency of stress concentration toward the axis of load is larger for gravel than for sand, especially the difference between the stresses on the axis of load for both systems is remarkable.

#### 4) Effect of loading form on stress distribution

Sinusoidal and quadratic forms were used as the wave pattern of dynamic load as already shown in Fig. 12. In case of the former it took some rise time to reach the peak value, while the latter reached instantaneously the peak. This means that the rate of loading is different with each other. As it was the aim to examine the influence of loading form, only the frequency of 1 cps was used.

The results are given in Fig. 12 for sand/sandy loam two-layered system. The influence of the loading form is not much recognized. In this case it is concluded that the difference between stress distributions due to the loading form is not observed as in the case of sandy loam.

#### 5) Stress attenuation along the axis of load

It is of importance in engineering practice to examine the stress attenuation along the axis of load in soil masses subjected to the dynamic load. In order to examine this and to compare the characteristics under the dynamic load with that under the static one, Fig. 14 is drawn using the logarithmic abscissa for stress, in which the static stress and the total stress under the sinusoidal and the quadratic waves are plotted, respectively. This shows that the tendency of stress attenuation is not affected by the sort of applied load and, in cases of sand and

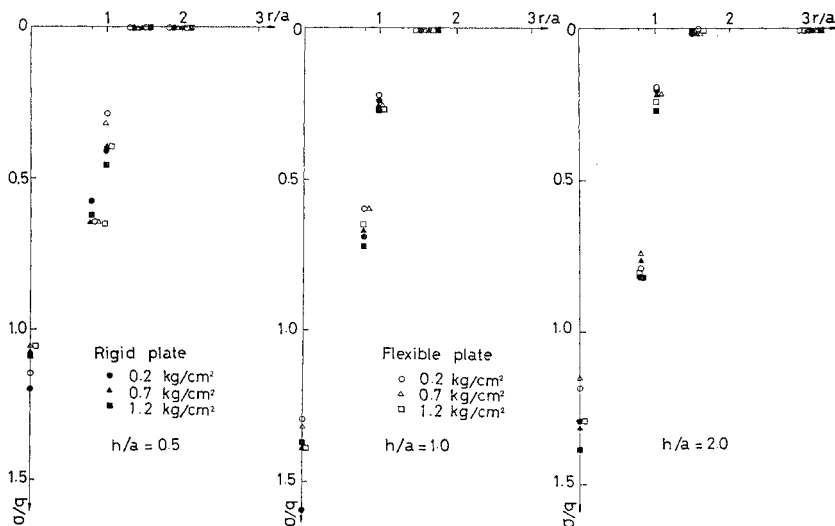


Fig. 13 Stress variation in two-layered (gravel/sandy loam) system due to the intensity of sustained load ( $z = 0.5a$ ).

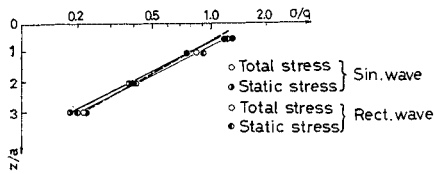


Fig. 14 Stress attenuation along the axis of load.

two-layered system, the stress decreases exponentially with depth.

## 5. FINITE ELEMENT ANALYSIS OF STRESS DISTRIBUTION IN SOIL MEDIUM

### (1) General

In recent year a great number of researches has been carried on with respect to application of the finite element method to the various boundary value problems.

The finite element method is very useful for practical purpose, so it becomes to be used widely as a mean of numerical computation in engineering fields. Also in soil mechanics this method is applied widely to the design and the analysis of various structures and foundations, not only by using various constitutive laws such as linear elastic, non-linear elastic, plastic and viscoelastic but also under various loading conditions.

The analysis is performed by assuming the continuum to be divided into finite number of elements. These elements are connected each other at nodal points, and a stiffness matrix relating the forces and the deflections at the nodal points is derived. Using the stiffness matrix  $[K]^e$ , the nodal forces  $[F]^e$  and the nodal deflection  $u$  of an element are connected with each other by the following equation.

$$[F]^e = [K]^e \{u\}$$

In axi-symmetric problem to which our present work corresponds, the nodal force signifies the compound force which is total one applying along the ring of an element.

### (2) Application of the finite element method to the model test

A soil medium of single-layered system in the test pit is divided into 168 ring elements with triangular cross section as shown in Fig. 15. The boundary conditions are expressed in the displacements of nodal points such that at the points on the axis of load there occurs no displacement in the radial direction and at the points on the bottom of the test pit the both radial and vertical displacements are not permitted.

The modulus of deformation of soil medium was

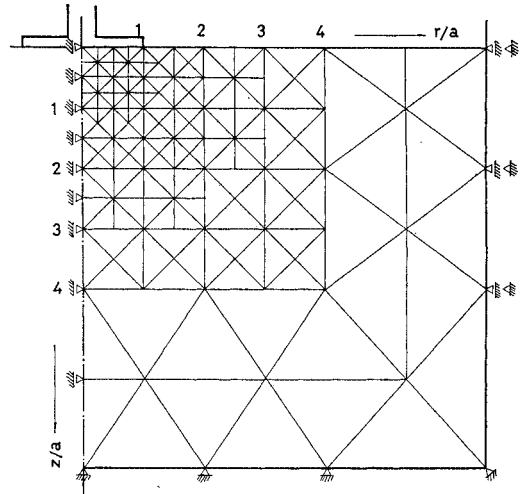


Fig. 15 Ring elements used in FEM-calculation.

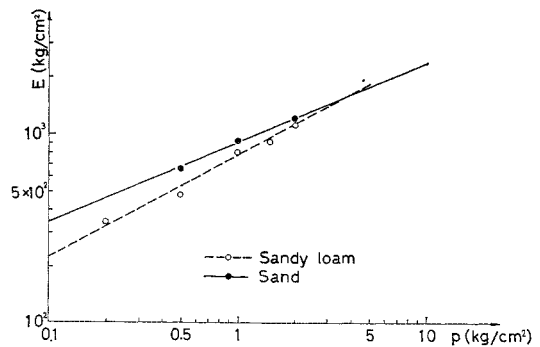


Fig. 16 Correlation between the modulus of deformation and the magnitude of confining pressure.

determined according to the experimental results of loading tests and also of a series of triaxial compression tests in the laboratory. Fig. 16 shows the correlation between the modulus of deformation and the magnitude of confining pressure in the latter tests. In this figure the value of the modulus of deformation corresponding to the range of confining pressure  $\sigma_c = 0.2-0.5 \text{ kg/cm}^2$  which may actually occur in the test pit is  $E = 330-520 \text{ kg/cm}^2$  for sandy loam and  $E = 460-600 \text{ kg/cm}^2$  for sand. Comparing these values with the results based on the loading test tabulated in Table 4, both are fairly well in agreement. The Poisson's ratio is assumed to be the value of 0.4.

**Table 4** Modulus of deformation based on the loading test

Distribution of contact pressure		Parabolic				Uniform			
Poisson's ratio		0	0.3	0.4	0.5	0	0.3	0.4	0.5
$E (\text{kg/cm}^2)$	Sandy loam	509	463	427	381	485	441	407	363
		596	543	501	447	568	517	477	426
	Sand	571	521	480	429	762	694	640	572
		576	523	484	432	768	695	645	576

The distributions of contact pressure at the loading plate were taken as uniform for the flexible plate and as parabolic form for the rigid one according to the measured results, respectively.

### (3) Result of computation

The numerical calculation was performed using FACOM 230-60 Computer in Kyoto University. Fig. 17 indicates the difference of stress distributions at various depths between the finite element method and the analytical solution based on the Boussinesq's

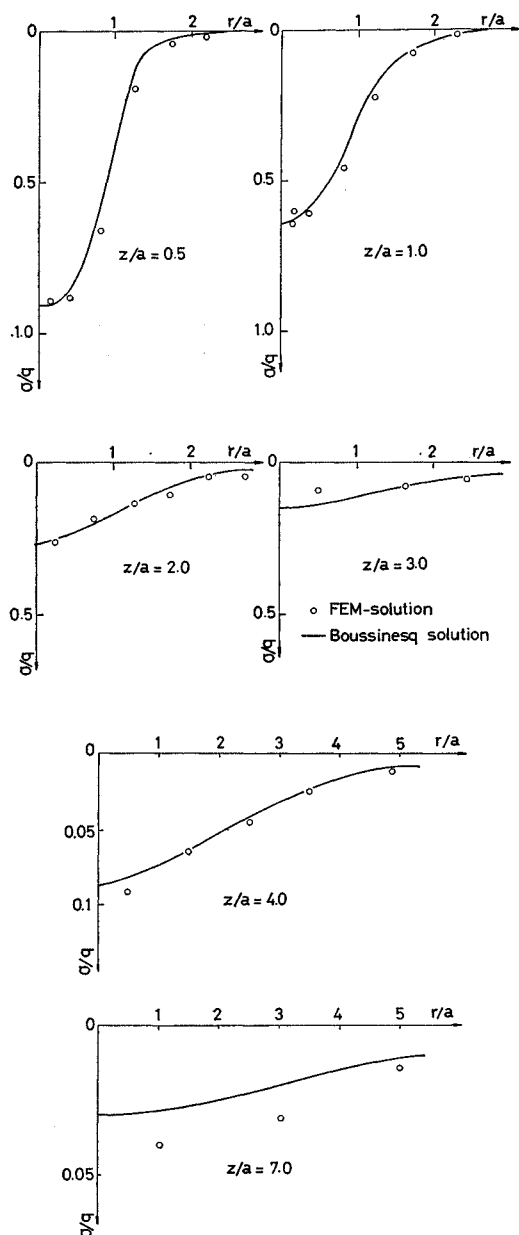


Fig. 17 Comparison of stress distributions computed by FEM and Boussinesq's solution.

equation. In this figure both results coincide with each other at shallow depths, *i.e.*,  $z=0.5a$ ,  $1a$  and  $2a$ , and the stresses computed by using the finite element method is larger than the other at the neighbourhood of the bottom wall of test pit. This is due to that both radial and vertical displacements of nodal points on the bottom of test pit are restricted in the finite element method. It may be considered, therefore, that the results of computation by using the finite element method are reliable.

## 6. CONCLUSIONS

A series of model tests on the stress distribution in the ground has been performed with respect to single or two-layered soil system. From the loading tests the following facts are mainly recognized.

- (1) Both sand and gravel have tendencies of stress concentration toward the axis of load, comparing with sandy loam.
- (2) Variation in stress distribution with load is larger in the range of small load intensity, and this is obvious at shallow depth and also on the axis of load.
- (3) In two-layered system the mechanical properties of soil material of the upper layer come to be marked with increase of the thickness of the upper layer.
- (4) The effect of dynamic loading on the stress distribution is remarkable in all loading tests. That is, the pattern of stress distribution becomes flatter under the dynamic loading compared with the static loading.
- (5) The influence of load frequency is not recognized at all within the range used during the loading test, *i.e.*, 0.5-5 cps. The effect of sustained load on the stress distribution is seen only at shallow depth.
- (6) Reaching the depth  $z=2a$  ( $a$ : the radius of loading plate), the stress distribution under dynamic loading agrees with that under static one. The depth to which the stress distribution is affected by the dynamic loading, however, may vary with the intensity of the dynamic load.

The authors would appreciate the assistance of Messrs. M. Yoneda and J. Yoshikawa through the experimental work. For instrumentation the authors are greatly indebted to Prof. S. Ichihara and Dr. K. Ueshita of Nagoya University in recommending new type of pressure cells.

## REFERENCES

- 1) Kögler, F. and A. Scheidig: Druckverteilung im Baugrunde, Bautechnik, Vol. 5, 1927, pp. 418-421.
- 2) Schleicher, F.: Zur Theorie des Baugrundes, Bauingenieur, Vol. 7, 1926, pp. 931-935.

- 3) Fröhlich, O.K. : Druckverteilung im Baugrunde, Springer, 1934, pp. 21-28.
- 4) Ohde, J. : Druckverteilung im Baugrund, Bauingenieur, Vol. 20, 1939, pp. 451-459.
- 5) Westergaard, H.M. : Stresses in Concrete Pavements Computed by Theoretical Analysis, Public Roads, Vol. 7, 1926, pp. 25-35.
- 6) Burmister, D.M. : The Theory of Stresses and Displacements in Layered Systems and Application to the Design of Airport Runways, Proc. Highway Research Board, Vol. 23, 1943, pp. 126-148.
- 7) Burmister, D.M. : The General Theory of Stresses and Displacements in Layered Systems III, J. Appl. Phys., Vol. 16, 1945, pp. 296-302.
- 8) Odemark, N. : Investigations as to the Elastic Properties of Soils and Design of Pavements According to the Theory of Elasticity, Statens Väginstitut, Stockholm, No. 77, 1949.
- 9) Lee, E.H. : Stress Analysis in Visco-Elastic Bodies, Quart. Appl. Math., Vol. 13, 1957, pp. 183-190.
- 10) Ishihara, K. and T. Kimura : The Theory of Viscoelastic Two-Layer Systems and Conception of Its Application to the Pavement Design, Proc. Sec. Int. Conf. Ann Arbor, Mich., 1967.
- 11) Sparrow, R.W. and A.C. Tory : Behavior of a Soil Mass under Dynamic Loading, J. ASCE, Vol. 92, No. SM-3, 1966, pp. 59-83.
- 12) Brown, S.F. and P.S. Pell : Subgrade Stress and Deformation under Dynamic Load, J. ASCE, Vol. 93, No. SM-1, 1967, pp. 17-46.

*(Received July 15, 1970)*

---